GAS FILLED HEAVY ION DETECTORS

H. Stelzer
GSI, Darmstadt

1. Historical Remarks and Introduction

Gas-filled detectors are, beside the anorganic scintillator, the oldest instruments to detect ionizing radiation. An ionization chamber was already used in the first experiments with cosmic rays in the beginning of this century. A major drawback of this instrument was the missing amplification device for the weak signal of an ion-chamber. It was not possible to record the pulse of a single ionizing event. In 1908 Rutherford and Hans Geiger published a paper (Rutherford 08) in which they described a device which was able to detect the single pulses of alpha particles. This first gas-filled detector which was able to record the pulses of individual ionizing events was in fact, in modern terminology, a proportional counter in cylindrical geometry. The internal gas-amplification was high enough that the single pulses of this counter could be directly recorded by a galvanometer. It was only in 1928 when Hans Geiger and W. Müller (Geiger 28) invented the nowadays called Geiger-Müller counting tube with its much higher internal gas gain. Here the gas multiplication around the thin wire of the tube is so high that even minimum ionizing particles like beta particles could be recorded without any further amplification. The pulse-height of such a Geiger-Müller counter is, as it is well-known, independent of the primary ionization, which is often a disadvantage. Only with the upcoming of vacuum tube amplifiers in the 1930's the advantage of a proportional counter or an ionization chamber, namely their proportionality between primary ionization and output pulse-height, could be fully exploited and came more and more into use. Nowadays, the Geiger-Müller counting tube is mainly of historical relevance, because the above mentioned non-proportionality between primary ionization and output signal and its long dead time in the order of a ms, but nevertheless, they are still in use for some special applications (Jones 81). One should point out that Geiger fully realized the importance of a high electric field in the gas amplification process and that such high fields could easily be produced around thin wires or sharp points (Geiger point counter (Geiger 12)). One may safely state that all the developments of gas-filled detectors with internal gas amplification is based on the pioneering work of Hans Geiger.

Another mile-stone in the evolution of gas-filled nuclear particle detectors is Charpak's invention of the multi-wire proportional chamber in 1968 (Charpak 68). He realized that each of thin parallel wires, spaced 2 mm apart and placed between two electrodes acting as cathodes, behaves like a proportional counter, essentially independent from each other. In this way large-area position sensitive detectors, especially needed in High Energy Physics, could easily be constructed. Within few years, nearly all electronic counter experiments in High Energy Physics, which used up to then mainly optical, acoustical or magneto-strictive spark-chambers as a position-sensing device, changed over to this new type of detector or to its close relative, the drift-chamber. It offered a much higher count-rate capability, shorter dead- and memory time and a

direct data-transfer into the computer, in contrast to optical data recording, just to mention a few of the numerous advantages of a MWPC. The rapidly growing use of multi-wire chambers is, of course, closely related to the development of modern solid state electronics in the 1960's.

The instrumentation in nuclear and heavy ion physics was dominated by solid state detectors (silicium- and germanium diodes), since their upcoming in the 1960's. To the experimentalist they offered unique advantages compared to the up to then mainly used proportional counters, ionization chambers and scintillation counters: an excellent energy-resolution, much better than obtained up to then, a linear response in the charged particle's energy, a high stopping power, which resulted in small size detectors, the possibility to produce very thin energy-loss detectors, the operation of the detector directly in the vacuum of the scattering chamber, and, especially important for those physicists who want to do more serious things than detector development, the easy availability off-the-shelf. A historical review of the development of semiconductor detectors is given by McKenzie (1979), who, together with D.A. Bromley, was one of the pioneers of this new detector technology.

With the beginning of the 1970's a interest in the physics of phenomena related to very heavy ions arose. New accelerators, like the UNILAC at the GSI at Darmstadt provided beams of projectiles as heavy as uranium. Now, in the spectroscopy of very heavily ionizing radiation, some serious drawbacks of the up to then so extremely successful semiconductor detectors became apparent. I will just mention them, without going into details: the pulse-height defect, the plasma time jitter, the degradation of the detector performance after exposure to intense radiation and their small size, which made it extremely costly to build large solid-angle detection systems. For these reasons, in many laboratories a new interest in gas-filled detectors arose. In the following I will try to illustrate the research which has been undertaken during the past decade on gas-filled counters for heavily ionizing radiation, by describing some specific examples.

II. Gas-filled Ionization Chambers

II.1 General Remarks

In an ionization chamber the electrons which have been deliberated by a nuclear charged particle in the sensitive gas-volume along the track of the particle are measured. The electric field, which separates the positive and negative charge-carriers, is either parallel or perpendicular to the particle's trajectory. It turns out that the number of produced electrons, to a high degree of accuracy, depends linearly on the energy the particle has lost in the gas-volume of the chamber. This holds true for a wide range of projectile charges and velocities. The linear response of a gas-filled ionization chamber means that there is a fixed mean energy required to create one electron-ion pair. This energy, usually denoted by W, amounts to about 30 eV for the commonly used counting gases and is about a factor of ten smaller for silicon detectors. The fact that W is practically independent of the particle's energy (at least above some hundred keV) comes about because the competition between ionization and excitation-processes is rather independent of energy and the amount of energy going

into kinetic energy of gas atoms is negligible Only at low energies at some hundred keV, the fraction of the energy-loss of the particle due to non-ionizing collisions increases, producing a corresponding increase in W, since there is less energy available for ionization processes.

However, one should bear in mind that the experimental evidence for the independence of W of the charge of the heavy-ion projectile is rather scarce (ICRU 79). The best thing then, and what is normally done, is to calibrate the ion-chamber with projectiles with known Z and energy. An energy-resolution as low as 0.7 % FWHM is routinely achieved, thus proving that the number of free electrons produced by a charged particle in a gas is an excellent means to determine the energy the particle has lost in the sensitive volume of the ionization chamber.

Basically two important parameters of a charged particle can be determined in an ion-chamber: 1. the total energy, when the particle is stopped in the chamber. 2. the nuclear charge Z, by measuring the energy ΔE the particle has lost on a certain path x and its total energy E. Very often gas-filled ion-chambers, especially small ones, are simply used as ΔE-counters, whereas the total energy is measured by silicon detectors mounted directly in the ion-chamber. Additionally, a gas-filled ionization chamber can be made position-sensitive by various methods, which I will discuss later. This feature is of special importance for large-size ion-chambers.

The main advantages of gas-filled ionization chambers, compared to solid-state detector telescopes, may be summarized as follows:

1. large size detectors can be built. In this way a broad range of the angular distribution of the emitted particles can be measured with one set-up. Furthermore the large solid-angle saves precious beam-time.
2. The response of an ion-chamber is essentially linear in the deposited energy. A pronounced pulse-height defect like in solid-state detectors is not observed, but recombination effects are obviously present. A heavy ion with a given energy yields a some percent higher signal, when the gas-pressure in the chamber is reduced by about a factor of two (but still high enough to stop the particle). This effect can not be explained by an electro-negative impurity.
3. no radiation damage occurs in the usually used counting gases like methane, iso-butane or tetrafluor-methane.
4. the dynamic range (i.e. the range of Z-values and energies which can be measured simultaneously) is much broader than of a solid-state detector telescope. Furthermore, the effective thickness (in mg/cm^2) of the detector can easily be adopted to the experimental requirements by simply changing the gas pressure.

All these points listed above are of special importance and relevance in heavy ion physics. The demands of experiments with heavy ions have triggered most of the recent developments of gas-filled ionization chambers.

II.2 A Modern Ion-chamber

In the following I will discuss, as an example of the state-of-the-art of modern ionization chambers, a chamber which is currently be assembled by our group (Gobbi 81) at GSI. An artist's view of the

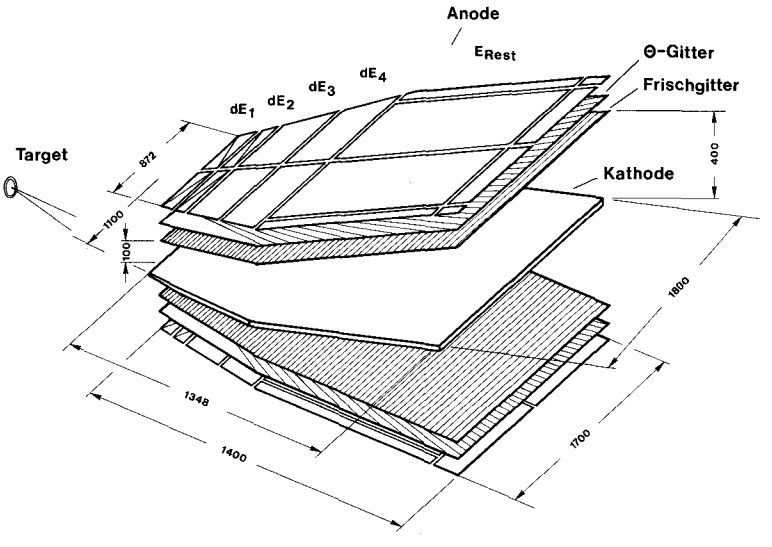

Fig. II.1 Perspective view of the Mammoth Twin ion-chamber.

Mammoth Twin ion-chamber is shown in Fig. II.1. The geometrical dimensions of the detector have been determined by two criteria: the demands of the experiments to be performed with this instrument and, on the other hand, the technical feasibility of this device.

This ion-chamber will be used in a new kinematic coincidence set-up for experiments with heavy ions with up to 20 MeV/u kinetic energy. In deep inelastic collisions, which will be further investigated with this apparatus, the projectile-like reaction products have nearly the projectile velocity, when the collision occured with a low Q-value. To stop heavy ions with this energy in hydrocarbon gases, one needs ~30 mg/cm² (for ^{238}U) and ~80 mg/cm² (for ^{20}Ne) (Huber 80). The active depth of the chamber has been chosen to 125 cm, which corresponds to a thickness of 9 mg/cm² per 100 mbar methane or 33 mg/cm² per 100 mbar iso-butane. With an operating gas-pressure of some hundred mbar, even the light and fast reaction products are stopped in the ion-chamber. Of course, a higher gas-pressure would reduce the necessary depth of the chamber, but there are several reasons against it:

- low energy particles would stop directly behind the entrance window and there always slight inhomogeneities of the electric field are present, which may cause incomplete electron collection by the anode.
- a higher gas pressure implies a thicker entrance window which causes more energy - and angle - straggling and a stronger support structure for the entrance window, which yields dead zones.
- it is still an open question wether at a higher gas pressure recombination effects do occur, at least for the heaviest ions. Again, a lower operating gas pressure is advisable.

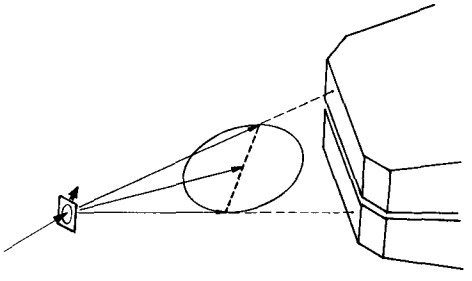

Fig. II.2 Sketch of the kinematics of a splitting process.

The general lay-out of the chamber is based on an earlier design (Sann 75). It is again a twin-chamber, but now the lower and upper half (fig. II.2) are completely independent detectors. The chamber body is made of ordinary structural steel, the interior is electroplated with nickel.

A massive iron-plate in the medium plane of the detector separates the gas-volume of the two ion-chambers and is strong enough to operate the upper and lower half at completely different gas-pressures. In this way particles with largely different energies can be measured simultaneously and the dynamic range is greatly increased. Such operating conditions are necessary, when one wants to investigate heavy ion reactions, where a high-energy forward emitted projectile-like fragment undergoes splitting. The resulting secondary fragments emitted in forward and backward direction within the moving frame of the primary particle are then observed at forward angles in the laboratory frame with significantly different energies, a kinematic situation which is sketched in fig. II.2. The relative angle of the two splitting fragments ranges from 0 to 60°. The entrance window of this twin ionization chamber is 800 mm wide (in the plane) and 2 x 100 mm high (out of plane). This dimension has been dictated by the technical feasability of the window.

Located 700 mm away from the target, the detector has an angular acceptance of ±30° (in the plane) which just fits to the above described splitting process. The distance of 700 mm of the entrance window to the target is dictated by the need of a reasonable long flight-path for time-of-flight measurements. The time stop-signal is provided by a large-area, but nevertheless very thin parallel-plate-avalanche counter, which is installed directly in front of the chamber. The massive plate in the medium plane (fig. II.3), which separates the upper and lower chamber, carries on both sides the cathode planes. The structure, which is ± 10° inclined to the medium plane, carries the anode plates, together with the Frisch-grid and the θ-grid.

The measurement of the energy the nuclear particle has lost across a given path (the width of the dE-plates) together with its total energy (equal to the sum of the signals on all anode plates) yields information about its nuclear charge. An optimum Z-resolution is obtained, when the ratio of $\Delta E : E_{total}$ is as high as .75 (Sistemich 76). The large dynamic range of the nuclear charges of the products from a heavy ion reaction requires a subdivision of the anode in several independent electrodes, which makes it possible to form the optimum $\Delta E : E_{total}$ ratio over the whole energy- and nuclear charge range. These considerations led us to the design of the anode shown in fig. II.1. There are four plates for the energy-loss measurement of the particle across the dE plates, which are 60, 60, 200 and 200 mm resp. wide. The last big plate determines the residual energy E_{Rest}. All the anode plates are split in two halves to lower the capacitance.

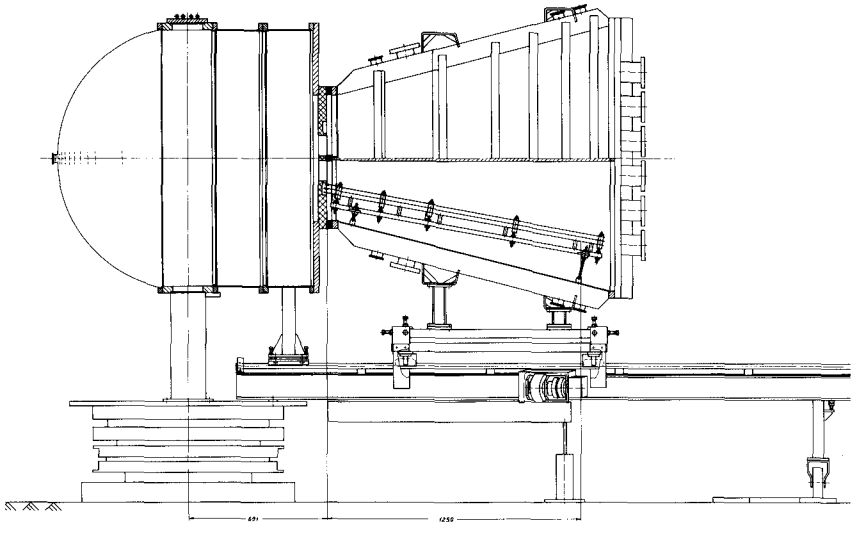

Fig. II.3 Side-view of the Mammoth ion-chamber with the scattering chamber.

The distance between the Frisch-grid and the anode is 40 mm. Between these two electrodes the so-called 0-grid is mounted. This grid consists of 50 μ wires which run parallel to the track of a particle coming from the target. The wire-spacing at the entrance window is 2 mm and at the chamber end 6 mm. This electrode determines the in-plane scattering angle. When the primary electrons drift to the anode, they induce a signal on the nearest wire when they pass through the 0-grid. All the wires are soldered to a discrete L-C-delay line and the wire which carries the signal is determined by measuring the time-difference between the signals at the two ends of the delay-line. With smaller chambers of this type, a position resolution of about 2 mm has been achieved by this method. The out-of-plane coordinate is measured via the time-difference between the passage of the charged particle through the chamber and the anode signal, since this signal only appears when the primary electrons have passed the Frisch-grid. This method to measure the Y-coordinate works of course only if there is a constant drift-velocity and hence a constant reduced field-strength E/p throughout the active chamber-volume. In earlier, smaller chambers, the time-difference between the cathode signal, which is prompt with the passage of the particle, and the anode signal was used to extract the Y-coordinate. But here in this big chamber the cathode signal will have a too slow rise-time to get out a reasonable timing information. Instead, the already mentioned parallel-plate avalanche counter placed in front of the ion-chamber will provide the timing. Another important aspect of this avalanche counter is to provide the fast trigger signal that a particle has hit the ion-chamber. All the signals of this chamber are rather slow, in the μs range, and, when using the ion-chamber in coincidence with other fast detectors, for example parallel-plate avalanche counters as recoil detectors, one would have to delay all the fast signals by some μs.

The cathode is on negative potential, the Frisch-grid is on ground, and the anode and the θ-grid are on positive potential. These last two are chosen such that no electrons are lost on the two grids. In the cathode Frisch-grid volume one needs a homogeneous reduced electric field strength of E/p = 1 V/(cm • Torr), when the chamber is operated with pure methane. At this field methane has a maximum drift velocity of 10 cm/μs. With one constant cathode potential all along the depth of the chamber, the electric field would fall off as 1/Y, Y being the cathode Frisch-grid distance, which varies between 100 and 400 mm. This strongly varying field not only influences the drift-velocity, a effect which deteriorates the position determination in the Y-coordinate, but has furthermore the desastrous effect that the primary electrons are not properly collected by the different dE anode plates.

The electric field and the potential distribution has been calculated with a computer program (Stelzer 82). A quite homogenoeus electric field with a correct collection of the primary electrons onto the different anode-plates can be achieved when the cathode is subdivided into segments. Each segment is on a potential according to its mean distance to the Frisch-grid. At the entrance, the first cathode segment is 4 mm wide, and each of the following is 4 mm wider than the preceeding one. Thus one needs about 23 different segments. Such a structure can easily be realized with printed-circuit material.

The chamber will be ready for the first test runs till the end of this year, the first experiments with this big detector are planned in spring 1983.

II.3 A new way to determine the in-plane scattering angle in an ion-chamber

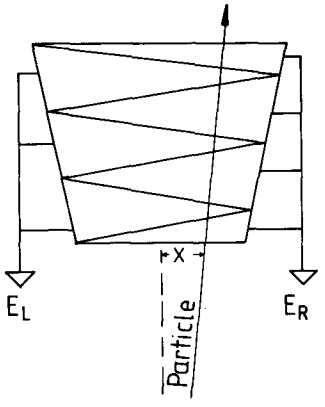

Fig. II.4 Position determination by the triangle method (Rosner 81).

Recently a new position measurement for ionization chambers has been reported by a group from the MPI Heidelberg (Rosner 1981). They cut the first ΔE-anode plate in triangles and connected the left and the right triangles of this saw-bladed structure to two amplifiers (fig. II.4). The energy-loss of a particle divides between left and right triangles according to the impact position x of the particle, and this impact position is given by the simple relation:

$$x = (E_R - E_L)/(E_R + E_L)$$

They report good linearity and obtained a position resolution of 0.3 mm with 132 MeV ^{32}S ions.

Our group (Gobbi 81) tried this method in our 120 cm deep ionization chamber and compared it with the position obtained with the above described θ-grid. This θ-grid method gives a sufficiently good position information (Δ x ~ 2 mm), but for short tracks, when the particle stops already after some cm, the resolution gets worse or the θ-signal is even missing. With the new method we did not achieve the good results reported by Rosner et al. We observed a 5% cross-talk, measured with a pulser between adjacent segments, which gets a big correction, when the signals on the left and right side are very different for large x . Furthermore, the specific ionization of the particle

increases along the path across this saw-bladed structure. In principle one can correct for this effect, but this makes the analysis more complicated. Finally, one should notice that this method needs twice the amount of electronics. Normally we use the θ-grid to determine the in-plane scattering angle, but for events with no θ-signal we apply the triangle method.

II.4 Bragg-Curve Spectroscopy

The most simple way to extract the information from an ionization chamber is to collect just all the electrons a nuclear charged particle has deliberated in the active gas-volume of the chamber on one anode plate. In this way the total energy the particle has spent in the chamber is measured. In addition to the total energy information about the nuclear charge of the particle can be obtained by determining the portion of energy the particle has lost over a given path-length x. This can be achieved by subdividing the anode into two or more seperately read-out plates, as it is done in the big chamber described in the preceding chapter. Even more detailed information about the nature of the particle and its physical properties can be obtained by determining the spatial distribution of the electrons produced along the path of the particle in the gas, i.e. if one measures the Bragg-curve. This Bragg-curve spectroscopy (BCS) has first been proposed and tested by C. Gruhn (Gruhn 79 and 82). Another BCS-detector with very interesting figures-of-merits has been built by a group of the TU Munich (Schiessl 82).

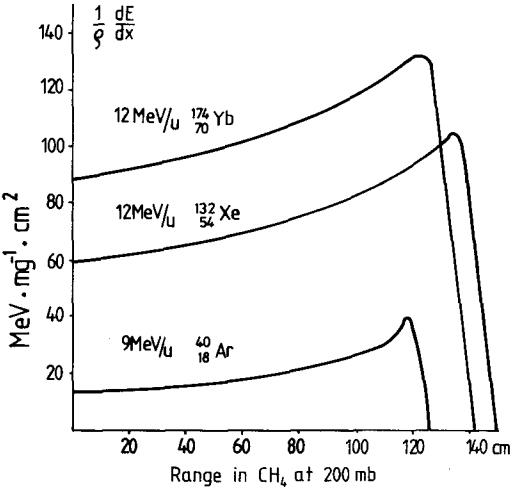

Fig. II.5 Bragg-curves of three different ions in methane at 200 mb.

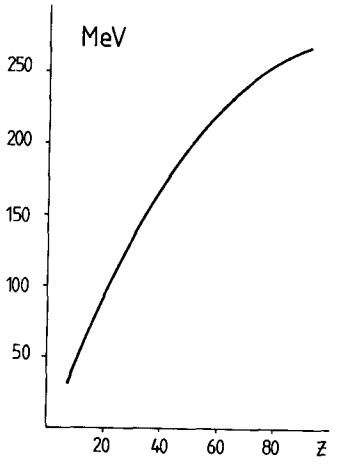

Fig. II.6 Energy-loss of a heavy ion with nuclear charge Z on its last 20 cm in methane at 200 mb.

Let me first try to point out why the Bragg-curve spectroscopy is a promising method to determine the energy and the identity of a heavy ion. In fig. II.5 are plotted the Bragg-curves of three different heavy ions, of Argon, Xenon and Ytterbium at 9 MeV/u and 12 MeV/u resp. The specific energy-loss is plotted versus the path length

of the heavy ion in methane at 200 mb. I have chosen this representation because, firstly, methane is our favourite ion-chamber gas due to its high drift-velocity and secondly, to illustrate the geometrical size of detectors needed to measure heavy ions at these energies. The enhancement of the Bragg-peak at the end of the path of the particle ranges from about 3 for the "light" heavy ion down to about 1.5 for the "heavy" heavy ion. The dE/dx-values in this figure and the following have been taken from the Northcliff-Schilling tables (Northcliff 70). What is actually measured is not the peak of the dE/dx-curve, but the energy the heavy ion has lost on its last portion of its range. By looking at fig. II.5, when one stays with methane at 200 mb as chamber gas, one sees that one should measure the energy the particle has lost on its last 20 cm. The energy a heavy ion with nuclear charge Z looses on its last 20 cm in methane at 200 mb is plotted in fig. II.6. The slope of this curve ranges from 4.8 MeV per nuclear charge at low Z-values down to around 1.6 MeV per nuclear charge at high Z-values. This means one needs an energy-resolution in the Bragg-peak of about 0.5 % to resolve single Z-values at high Z, which is certainly not easy to achieve.

How has such a BCS-detector been realized by the two groups? Both ionization chambers have the electric field lines parallel to the particle track. The collection of the electrons along the particle track has the inherent disadvantage that now the charge carriers are in close neighbourhood for a much longer time than in a configuration where the electric field is perpendicular to the track. Recombination effects may lead, at least for very heavily ionizing particles, to a loss of electrons. A schematic view of the detector of the Munich group is shown in fig. II.7.

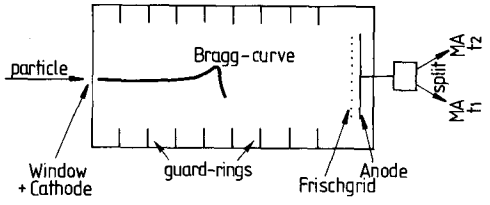

Fig. II.7 BCS-detector of the Munich group (Schiessl 82).

The entrance window serves as the cathode, which is on ground potential. The electrons the particle has produced in the gas drift to the anode and are sensed by the amplifier when they have passed the Frisch-grid. The chamber is 16 cm deep. The separation of the ionization in the Bragg-peak from the total ionization is done by a simple trick: the preamplifier output signal is split and fed into two main-amplifiers with different shaping times t_1 and t_2. T_1 is about the collection time of the electrons from the Bragg-maximum and the signal from this main-amplifier is thus proportional to the ionization around the Bragg-peak, and, as we have seen from fig. II.6, is therefore a unique function of the nuclear charge. The shaping time t_2 of the second amplifier is chosen to be longer than the total collection time of the electrons and is thus proportional to the total energy.

Both groups report a Z-resolution of about 1.2 % at Z = 16 (Schiessl 82) and at Z = 26 resp. (Gruhn 82). This figure-of-merit is about the same as the one achieved with 'conventional' ion-chambers, where the electrons are collected perpendicular to the track and the nuclear charge is determined by a ΔE-E_{Rest} measurement on two anode plates. This method works best, as already mentioned, when ΔE and E_{Rest} have about the same magnitude, and under this optimum condition, a Z-resolution of 1.1% at Z = 92 has been achieved (Sann 80). But, since the length of the anode plates is fixed, this optimum condition is only fulfilled in a rather limited energy- and Z-range. By principle of operation, a BCS - detector always takes the optimum part of the ionization track

as the Z-signal and thus should have a much bigger dynamic range with good Z-resolution.

One way to take advantage of the Bragg-peak measurement in an ion-chamber with the electric field lines perpendicular to the track would be to divide the anode in 10 cm wide plates. The two or three last anode plates which show a signal will be added together and taken as the Bragg-peak signal (cf. fig. II.5,6). Combined with the measurement of the total energy by summing up all the anode plates, this should yield an optimum Z-resolution over a wide dynamic range. A chamber with 140 cm depth would need 14 preamplifiers, mainamplifiers and ADC channels; an amount of electronics still tolerable.

III. Low-Pressure Proportional Counters

III.1 Parallel-Plate-Avalanche Counters

Since their upcoming in the instrumentation technique for heavy ion experiments in 1975 (Hempel 75, Stelzer 76), parallel-plate avalanche counters (PPAC) have found wide-spread use predominantly as timing detectors for heavily ionizing radiation. Its simple design and operation, its excellent timing results (a time-resolution of 120 ps (FWHM) is obtained with a small size detector, for large-area detectors a time-resolution of 200-300 ps FWHM is routinely achieved under experimental conditions) and its reliability are one of the main attractive features of this gas proportional counter. Very soon a PPAC could be made position-sensitive by inserting a grid of wires between the anode and cathode and by dividing the cathode into stripes (Breskin 77, Eyal 78, Just 78, Harrach 79).

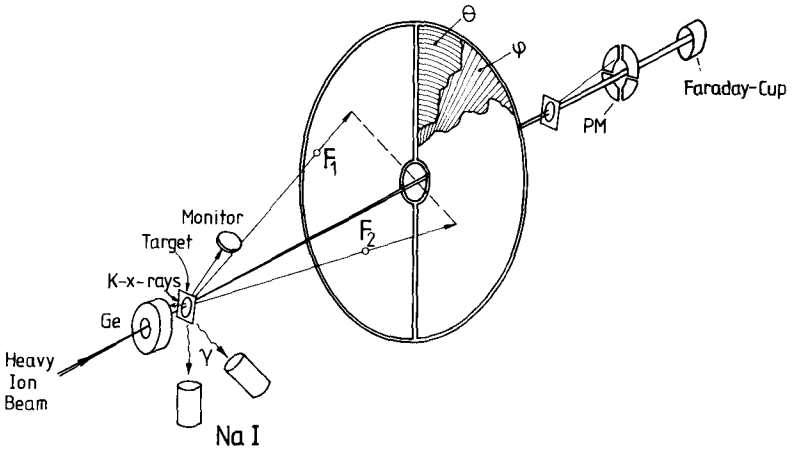

Fig. III.1 Experimental set-up with a ring-counter (Bock 82).

As an example of the great flexibility one has in the design of a PPAC I would like to mention the ring-counters (Gaukler 77) which have been built in the last years in our detector laboratory (Bock 82, Lieb 82). The cathode made of printed-circuit material has a etched ring pattern; the rings are read out by means of a tapped delay-line and thus the scattering angle θ of the particle is directly determined. The azimuthal

angle φ is obtained by inserting a grid of wires, with the wires in radial direction, between anode and cathode; if only a rough φ-determination is needed, the subdivision of the anode-foil into azimuthal segments will do the job. The counter has a hole in the middle to let the beam pass through. A typical experimental configuration with such a ring-counter is shown in fig. III.1 (Bock 82). The two reaction-products from a binary reaction of the beam in the target are detected in the ring-counter, which measures their scattering angles and their time-of-flight-difference. These quantities completely determine the kinematics of the binary reaction. The sodium-iodide crystals around the target measure the accompaning γ-rays. The counters denoted by PM monitor the beam position.

A problem specifically met in heavy ion physics is the wide dynamic range of the specific ionization dE/dx of the particles to be detected. Sometimes particles have to be registered which differ in their energy-deposit in the gas of the PPAC by more than a factor of 100. In an experimental environment with a high flux of very heavily ionizing radiation the high-voltage applied to the PPAC has to be lowered by about 10 or 20 volts to avoid sparking, and 100% detection efficieny for light particles, e.g. α-particles, is no longer achieved. We found out a simple trick to improve the dynamic range of the detection efficiency of a PPAC by simply increasing the operating pressure from the usual 10 mb to about 30 mb. Obviously, at this higher pressure a self-quenching effect in the gas-multiplication process occurs. In fig. III.2 is plotted the pulse-height ratio R for fission fragments and α-particles from a ^{252}Cf-source versus the operating gas-pressure. The small-size PPAC with a 0.8 mm anode-cathode gap shows at a low pressure a pulse-height ratio of about 90, a value one expects from dE/dx tables (Northcliff 70) and levels off to about 10 at > 40 mb pressure. The large-size detector with a 2 mm gap exhibits already at low pressure a strong quenching effect. A ratio of ~ 30 has also been observed by other groups (Hempel 75, Just 78). Above 25 mb the pulse-height ratio of fission fragments and alpha-particles is independent from the gas-pressure and is about 6. Our group (Gobbi 81) has already often made use of this feature of a PPAC. "Light" heavy ions are efficiently suppressed by operating the PPAC with a low pressure and a reduced high-voltage, whereas at a higher pressure and increased HV all the light ions are registered with full efficiency.

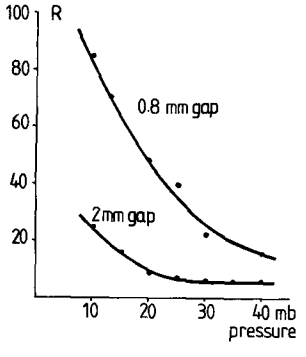

Fig. III.2 Quenching in a PPAC (cf. text).

A French group (Urban 81) investigated the response of a PPAC with a 5 mm gap at 100 mb i-butane to minimum-ionizing particles, which have a specific ionization a factor of 1000 smaller than α-particles at 5 MeV. In a planar electrode configuration it is not possible to maintain at 100 mb pressure the high electric field one needs to multiply sufficiently high the few primary electrons the particle has left behind in the detector. The maximum attainable reduced field strength is 80 V/(cm • mb), about a factor of five to six smaller than normally reached in low-pressure counters. The efficiency is thus only 80%, the time-resolution is 3.7 ns (FWHM).

As long as we use PPAC's in our laboratory, there is a discussion about the question whether the very low energy secondary electrons emitted by the heavy ion traversing the cathode foil contribute to the signal. These electrons which are produced

directly at the cathode are most important for a timing measurement, since they have always a constant drift-time and by far the biggest gas-multiplication across the whole anode-cathode gap (according to the Townsend-law of the gas-multiplication process). The yield of secondary electrons depends on the specific energy-loss of the heavy ion and ranges typically between some ten and some hundred in the forward direction (Pferdekämper 77). The yield of primary electrons due to ionization in 1 mm i-butane at 10 mb is roughly about a factor of 20 higher, thus outnumbering completely the secondary electron emission process. One could think of evaporating the cathode with a substance, like lithium-fluoride, to enhance the secondary electron yield. Tests with such a counter are planned in our laboratory in the near future.

III.1 The Double-grid Avalanche Counter

Following the idea of Charpak's multi-step-avalanche chamber, where the overall multiplication process is subdivided into two steps (Charpak 78, Breskin 79), one of us (Lynen 80) suggested to use this principle of operation in a very low pressure heavy ion detector. The schematic view of such a double-grid-avalanche counter (DGAC) is shown in fig. III.3. The detector consists of four electrodes, denoted by S, K, A and T. S and T are thin mylar foils (1.5 µm) or stretched polypropylen foils (0.6 µm) uniformly evaporated either with silver or gold.

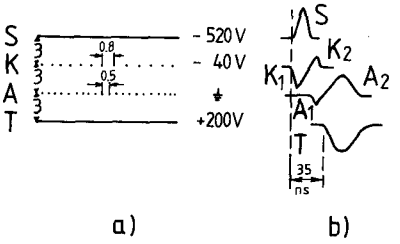

Fig. III.3 Schematic view of a double-grid avalanche counter.
a) electrode configuration.
b) shape of the observed signals.

The operating gas-pressure is 2 mb i-butane. The electrodes K and A are orthogonal wire grids of 20 µm gold-plated tungsten wires. The wire-spacing is 0.8 mm on the K-electrode and 0.5 mm on the A-plane. The spacing between adjacent electrodes is 3 mm. Typical potentials applied to the different electrodes are indicated in fig. III.3 as well. Fig. III.4 shows a plot of the electric field lines in such a configuration (Stelzer 82). One distinguishes three regions with quite a different field strength. In the high field region between S and K a reduced field-strength E/p = 800 V/(cm • mb) is reached, nearly twice as high as normally achieved in PPAC's. In this gap the main amplification process occurs. Most of the secondary electrons are caught by the wires of the K-grid and there a fast (rise-time 3ns) negative signal (labelled K_1 in fig. III.3b) appears, which induces on S a fast positive signal. Close in the vicinity around a wire of the K-plane, in the very high field region, most probably a second amplification occurs, as already pointed out by Breskin (1982). The rest of the electrons drift into the low-field region K-A with E/p = 150 V/(cm • mb), where only little gas-amplification occurs. Practically all the electrons pass through the A-grid and reach the medium-field region A- T (E/p = 300 V/(cm • mb)), where again multiplication takes place. A rather slow negative signal with a rise-time ~ 12 ns appears on T, which induces a positive signal A_2 on the A-grid. The signal-component A_1 most probably comes from electrons caught by the A-plane, which induces the K_2-component on K. The signal on T is 35ns later than the signal on K

and S. This time-difference can be used to estimate the drift-velocity of electrons in iso-butane at these high E/p values. The distance between K and T is 6 mm, hence the drift-velocity is 17 cm/μs, about a factor of three higher than at low E/p values (Bohrmann 76).

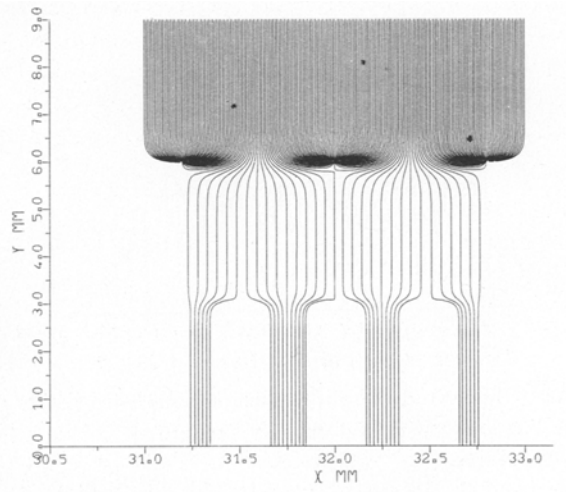

Fig. III.4 Electric field lines in a DGAC. Electrode 'S' is located at Y=9 mm. Potentials as in Fig. III.3.

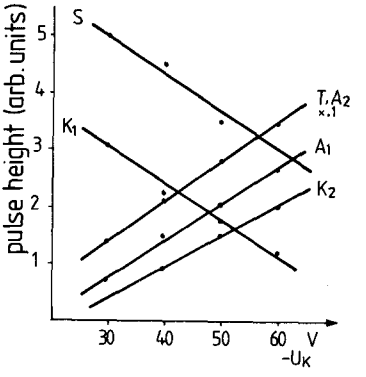

Fig. III.5 The signals of a DGAC as a function of U_K.

This qualitative picture of the gas-amplification process and of the development of the signals on the different electrodes has been gained by studying the pulse-height and the pulse-form of all the signals as a function of the potentials applied to the four electrodes. Fig. III.5 shows the pulse-height of the signals as a function of the potential U_K applied to the K-grid. This plot clearly shows the mutual dependence and correlations of all the signals. A more negative potential on K decreases the field between S and K, but increases the field in the second amplification gap.

All the signals are in the order of some mV and, after a fast, low-noise amplifier, they all show an excellent signal-to-noise ratio. The signal from the S-electrode is taken as a timing-signal. The measured timing peak of the light fragments of a ^{252}Cf source has a width of 400 ps (FWHM). Taking into account the intrinsic velocity-distribution of these fragments, their energy-loss-straggling in the foils of the preceding start-counter and the contribution of the start-counter, one calculates a time-resolution of the DGAC (active area 20 x 30 cm²) of 200 ps (FWHM). By looking at the field-line distribution of such a counter (fig. III.4) one should expect a strong variation of the driftpath-length and hence of the drift-time of the electron to the nearest wire of the K-grid, depending on the impact point of the nuclear particle on the counter. But due to the transversal diffusion of the electron cloud on their way to the K-grid, these driftpath differences are smeared out. The transversal diffusion of the electrons during their drift through the 3 mm S - K gap can be estimated as follows:

1. at atmospheric pressure, at low E/p values, the transversal diffusion is (Jean-Marie 79): δx = 235 μm per 10 mm drift

2. the diffusion scales with 1/SQRT(p) at constant E/p (Farr 78)
   Neglecting the E/p dependence, one gets at p = 2 mb:
   - ϑ x = 0.235 • SQRT(500) • 0.3 mm FWHM
   - ϑ x ~ 1.60 mm FWHM.

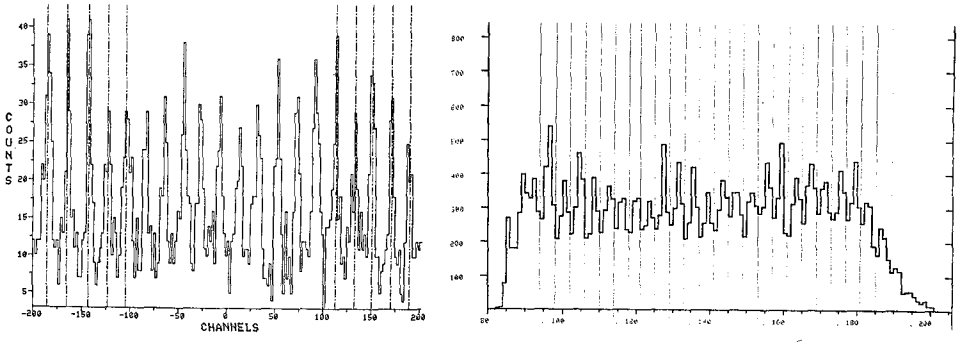

Fig. III.6 a) Position spectrum of a DGAC (illiminated roughly homogeneous with elastically scattered 5.9 MeV/u Xe-ions) with a 4 mm tap structure.
b) the same for a DGAC with 2 mm taps.

The grids K and A are used for the position determination in the two coordinates. The wires are grouped in 4 mm wide bins and soldered together to a tapped

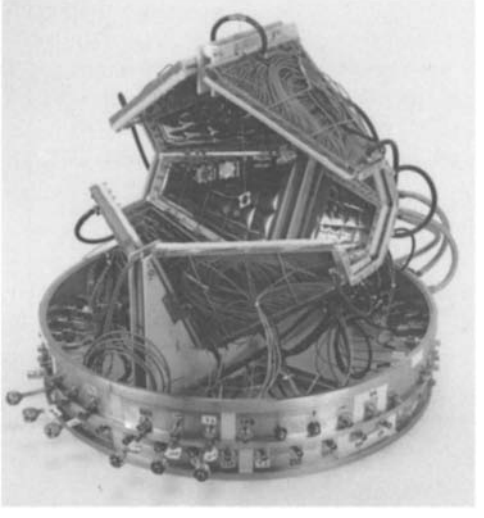

Fig. III.7 Experimental arrangement of 10 DGAC's around the target (Lynen 82).

Fig. III.8 Installation of DGAC's in a big scattering chamber (Gobbi 81).

Fotos: A. Zschau, GSI

delay-line. As delay-line we use either 3 ns per tap long Lemo-cables or chips. The delay-line is read out at both ends, a method which allows a rough interpolation between two taps. Furthermore, since the sum of the two signals has to be a constant, namely the total length of the delay-line, multi-particle hits on the detector can be

clearly distinguished. Fig. III.6a shows a position spectrum of 5.9 MeV/u Xe-ions, elastically scattered on Au; the 4 mm wide tap structure is clearly resolved. This shows that the diffusion of the electron cloud is less than 4 mm. Fig. III.6b shows the position spectrum of another detector which has a 2 mm wide tap structure; here the tap structure is much less resolved, which indicates a transversal diffusion in the order of 2 mm, in fair agreement with the above estimated value.

The signal from the T-electrode (cf. fig.III.3) is well suited for an energy-loss measurement. The resolution is in the order of 25%.

Due to the low operating pressure of 2 mb, even large-size (20 x 30 cm^2) DGAC's can be built which have only 10 mm wide frames. These frames are permanently glued together and are thus gas-tight and do not need an extra housing to contain the counting gas. This has the very important advantage that these counters can be installed very close together, thus minimizing dead spaces between them. A further advantage of the low pressure is that the S and T-electrode can serve as well as the gas-windows, which considerably reduces the total thickness of the counter, without deterioating too much the time- and energy-loss resolutions.

These double-grid avalanche counters have been built by our group since 1981 for two large experimental set-ups:

1) for experiments at the SC at CERN with 84 MeV/u carbon-ions, 10 DGAC's in trapezoidal form (active area 220 cm^2), were arranged around the target to detect the light and heavy fragments (Lynen 82). The dynamic range is wide enough to register with full efficiency light ions A > 10 in the presence of heavy target-residues. Fig. III.7 shows the experimental arrangement.
2) Twelve 20 x 30 cm^2 counters of this type have been built for a new kinematic coincidence set-up for experiments at 20 MeV/u at the upgraded UNILAC (Gobbi 81). Fig. III.8 shows the installation of the counters inside the scattering-chamber.

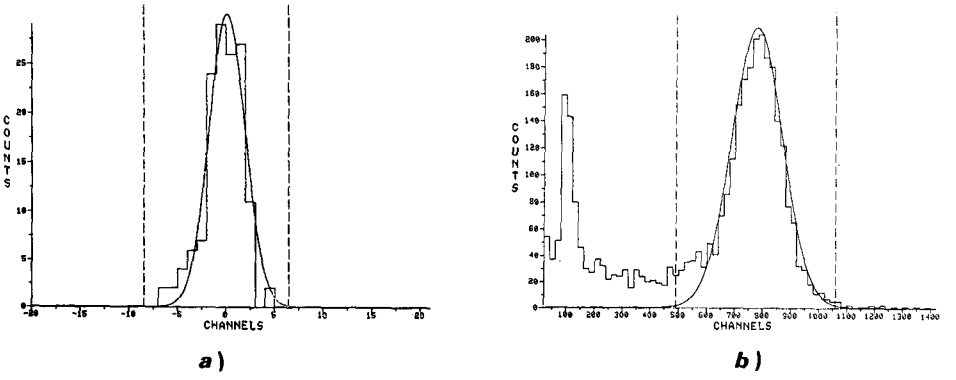

Fig. III.9 a) Time resolution of a DGAC (cf. text). (1 ch = 100 ps). b) Pulse-height spectrum of elastically scattered Xe-ions in a DGAC.

These briefly mentioned set-ups have already been used sucessfully in several experiments. Fig. III.9a shows the performance of the timing of a DGAC. In this figure the difference between calculated and measured time is plotted. The calculated time has been obtained from the scattering angles of elastically scattered Xe on Au at 5.9 MeV/u. The time spectrum shown includes the contribution from the uncertainty in the

angle-determination (due to the 4 mm position-resolution in the DGAC's and the 4 mm wide beam spot).

Fig. III.9b shows the pulse-height spectrum in a DGAC of Xe-ions from the above reaction. Events below the dashed line at channel 500 are background events.

Quite recently a small-size DGAC (5 x 7 cm^2) has been built and tested (Keller 82), which differs in some aspects from the above described ones:

1) The wire distance in the K- and A-plane is 1 mm.
2) The A-T gap has been increased from 3 to 6 mm.
3) Two neighbouring wires are soldered together to a tap of a delay-line, i.e. the tap width has been decreased from 4 mm to 2mm.

Let me briefly describe the main differences in the performance of this new designed DGAC compared to the old one:

1. Despite the increased wire distance of 1 mm (instead of 0.8 mm) in the K-plane, the counter still has an excellent time-resolution of <200 ps (FWHM), as determined with a ^{252}Cf-source and a 1.4 MeV/u Kr-beam. This effect can be understood by remembering the estimated transversal diffusion of ~1.6 mm of the electrons (see above) across the 3 mm wide gap. Fig. III.10a shows a time-spectrum

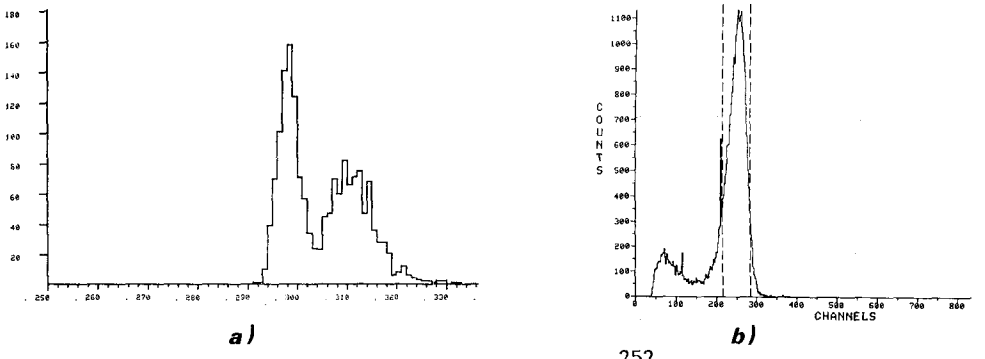

Fig. III.10 a) TOF-spectrum of the fragments of a ^{252}Cf-source between a small-size PPAC and a DGAC (1 ch = 100 ps).
b) Pulse-height spectrum of 1.4 MeV/u Kr-ions. The resolution is ~20 %. (The spikes at channels 120 and 220 are pulser signals.)

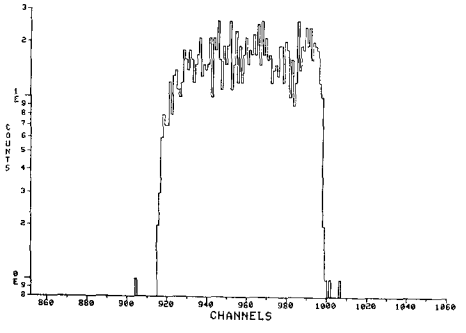

Fig. III.11 Position spectrum of 1.4 MeV/u Kr-ion in a DGAC (cf. text).

of the light and heavy fragments of a ^{252}Cf-source. The observed width of 400 ps (FWHM) includes the velocity- and energy-loss straggling in the start-counter and the contribution of the start-counter (a small-size PPAC) itself. The total thickness of the counter is <300 µg/cm^2 (the entrance window, the S-electrode and the T-electrode; all are stretched polypropylene foils with some silver-coating). It would be highly desirable to reduce the thickness furthermore. One way to do that would be to replace the S-foil by a narrow grid of wires. But now it is doubtful wether the good timing properties are still

maintained. The primary electrons produced directly at S (acting as cathode, cf. fig. III.3), which are most important for the timing properties of the detector, experience an inhomogenous electric field, since at the beginning of the drift to the anode, there is no smearing-out effect due to a diffusion process.

2) Due to the bigger A-T gap, the signals on A and T are now completely decoupled. The signal on A is now negative, caused by electrons caught by the wires and is no longer a positive signal induced by T. This offers the possibility to adjust the pulse-height on T (for example, to match the pulse-height to the range of the charge-sensitive ADC which measures the energy-loss) without affecting the signal on A. Fig. III.10b shows the pulse-height spectrum of 1.4 MeV/u Kr-ions.
3) The effect of the reduced tap-width of 2 mm on the position determination has already been discussed (fig. III.6). Fig. III.11 shows the position-spectrum measured on the K-grid when the detector is illuminated with 1.4 MeV/u Kr-ions through a circular mask with 5.5 mm diameter. In the Y-coordinate a narrow cut has been applied. From the sharp slope at the edges of the mask a resolution of o.25 mm (FWHM) is calculated. On the Y-coordinate, the A-grid (cf. fig. III.3), the position resolution is a factor of two worse. This finding can be explained by the longer drift-path of the electrons through the detector and hence a bigger transversal diffusion. On this detector commercially available delay-line chips have been used. Two types (BELFUSE and RHOMBUS) have been tested and compared. They showed similar performance. The linearity of these delay-lines is good enough for a position-resolution of about 2 mm, but certainly not adequate for a resolution of <1 mm.

IV. Summary and Outlook

I have tried to illustrate the present status of gas-filled heavy-ion dedectors. Despite their venerable age, gaseous detectors are in a still ongoing stage of development, continously modified and adapted to new experimental requirements. Heavy ion experiments require detection systems which are able to record simultaneously in only one detector several parameters, like time-of-arrival, position or energy, of particles covering a broad range of specific ionization. Gas-filled detectors have proven to be well suited to meet these demands.

In the near future, the interest in heavy-ion physics will focus on higher energies and the demands for detectors will change. On the one hand, very thin detectors, like the one used up to now, will be needed to register particles from the target-fragmentation region, but the fast forward-going products with their much less specific ionization and their high multiplicity will require detection systems which resemble more and more the ones used in High Energy Physics.

I thank all my colleagues for the many helpful discussions during the preparation of this manuscript, especially Dr. A. Gobbi and Prof. U. Lynen.

Literature

Bock 82: R. Bock, Y.T. Chu, M. Dakowski, A. Gobbi, E. Grosse, A. Olmi, H. Sann, D. Schwalm, U. Lynen, W.F.J. Müller, S. Bjornholm, H. Esbensen, W. Wölfli, E. Morenzoni, accepted for publication in Nucl. Phys.

Bohrmann 76: S. Bohrmann, Diplomarbeit, Universität Heidelberg, 1976, unpublished

Breskin 77: A. Breskin, and N. Zwang, Nucl. Instr. & Meth. 146(1977)461

Breskin 79: A. Breskin, G. Charpak, S. Majewski, G. Melchart, G. Petersen, and F. Sauli, Nucl. Instr. & Meth. 161(1979)19

Breskin 82: A. Breskin, Nucl. Instr. & Meth. 196(1982)11

Charpak 68: G. Charpak, R. Bouclier, T. Bressani, J. Favier, and C. Zupancic, Nucl. Instr. & Meth. 62(1968)262

Charpak 78: G. Charpak, and F. Sauli, Phys. Lett. 78B(1978)523

Eyal 78: Y. Eyal, and H. Stelzer, Nucl. Instr. & Meth. 155(1978)157

Farr 78: W. Farr, J. Heintze, K.H. Hellenbrand, and A.H. Walenta, Nucl. Instr. & Meth. 154(1978)175

Gaukler 77: G. Gaukler, H. Schmidt-Böcking, R. Schuch, R. Schule, H.J.Specht, and I. Tserruya, Nucl. Instr. & Meth. 141(1977)115

Geiger 12: H. Geiger and E. Rutherford, Phil. Mag. 24(1912)618

Geiger 28: H. Geiger and W. Müller, Phys. Z. 29(1928)839 and Phys. Z. 30(1929)489

Gobbi 81: A. Gobbi, G. Augustinski, R. Bock, H. Daues, S. Gralla, K.D.Hildenbrand, M. Ludwig, W.F.J. Müller, A. Olmi, M. Petrovici, W. Quick, H.Sann, H. Stelzer, J. Toke, GSI Scientific Report 1981

Gruhn 79: C.R. Gruhn, in: Proc. Symposium on Heavy Ion Physics from 10 to 200 MeV/u, BNL-51115(1979), p. 471

Gruhn 82: C.R. Gruhn, M. Binimi, R. Legrain, R. Loveman, W. Pang, M. Roach, D.K. Scott, A. Shotter, T.J. Symons, J. Wouters, M. Zisman, R. Devfries, Y.C. Peng, and W. Sondheim, Nucl. Instr. & Meth. 196(1982)33

Harrach 79: D.v. Harrach, and H.J.Specht, Nucl. Instr. & Meth. 164(1979)477

Hempel 75: G. Hempel, F. Hopkins, and G. Schatz, Nucl. Instr. & Meth. 131(1975)445

Huber 80: F. Huber, A. Fleury, R. Bimbot, D. Gardes, Ann. Phys. Fr. Vol. 5(1980)

ICRU 79: International Commission on Radiation Units and Measurement, ICRU Report 31(1979)

Jean-Marie 79: B. Jean-Marie, V. Lepeltier, and D. L'Hote, Nucl. Instr. & Meth. 159(1979)213

Jones 81: A.R. Jones and R.M. Holford, Nucl. Instr. & Meth. 189(1981)503

Just 78: M. Just, D. Habs, V. Metag, and H.J. Specht, Nucl. Instr. & Meth. 148(1975)283

Keller 82: J.G. Keller, K.-H. Schmidt, Ch. Sahm, and H. Stelzer, to be published in Nucl. Instr. & Meth.

Lieb 82: K.P. Lieb, S. Brüssermann, H. Emling, E. Grosse, J.Stachel, and P. Sona, to be published

Lynen 80: U. Lynen, private communication

Lynen 82: U. Lynen, R. Bock, Y.T. Chu, P. Doll, R. Glasow, A. Gobbi, K.D. Hildenbrand, H. Ho, W. Kühn, H. Löhner, W.F.J. Müller, A. Olmi, D. Pelte, H. Sann, R. Santo, H. Stelzer, U. Winkler, invited talk at the Int. Conf. on Selected Aspects of Heavy Ion Reactions, Saclay, May 3-7, 1982, Nucl. Phys. A387(1982)129

McKenzie 79: McKenzie, Nucl. Instr. & Meth. 162(1979)49 and references therein

Northcliff 70: L.C. Northcliff, and R.F. Schilling, Nucl. Data Tables A7(1970)

Pferdekämper 77: K.E. Pferdekämper, and H.G. Clerc, Z. Physik A280(1977)155

Rosner 81: G. Rosner, B. Heck, J. Pochodzalla, G. Hlawatsch, B. Kolb, and A. Miczaika, Nucl. Instr. & Meth. 188(1981)561

Rutherford 08: E. Rutherford and H. Geiger: Proc. Roy. Soc. Lond., Ser. A81(1908)141

Sann 75: H. Sann, H. Damjantschitsch, D. Hebbard, J. Junge, D. Pelte, B. Povh, D. Schwalm and D.B. Tran Thoai, Nucl. Instr. & Meth. 124(1975)509

Sann 80: H. Sann, private communication

Schiessl 82: Ch. Schiessl, W. Wagner, K. Hartel, P. Kienle, H.J. Körner, W. Mayer and K.E. Rehm, Nucl. Instr. & Meth. 192(1982)291

Sistemich 76: K. Sistemich, P.Armbruster, J.P. Boucquet, Ch. Chauvin, and Y. Glaize, Nucl. Instr. & Meth. 133(1976)163

Stelzer 76: H. Stelzer, Nucl. Instr. & Meth. 133(1976)409

Stelzer 82: this programm is based on: H. Buchholz, Elektrische und magnetische Potentialfelder, Springer-Verlag, Berlin 1957. It has originally been written to calculate field distributions in drift-chambers and multiwire proportional chambers (cf. K. Bethge (ed.) Experimental Methods in Heavy Ion Physics, p. 167. Lecture Notes in Physics, Vol. 83, Springer-Verlag 1978).

Urban 81: M. Urban, W.R. Graves, and C. Heil, Nucl. Instr. & Meth. 188(1981)47